Pergamon

Int. J. Heat Mass Transfer. Vol. 40, No. 2, pp. 269–280, 1997

0017–9310/97 $15.00 + 0.00

PII: S0017-9310(96)00134-2

Thermal conductivity of polyimide foams

ROLAND CAPS, ULRICH HEINEMANN and JOCHEN FRICKE
Bayerisches Zentrum für Angewandte Energieforschung e.V. (ZAE Bayern), Am Hubland, D-97074 Würzburg, Germany

and

KARL KELLER
ESA estec, Postbus 299, 2200 AG Nordwijk, The Netherlands

(*Received* 21 *November* 1995 *and in final form* 26 *March* 1996)

Abstract—Measurements of the thermal conductivity of polyimide foams have been performed in the temperature range 173–323K for different gas pressures and different gas types (CO_2 and Ar). The extinction of thermal radiation has been determined by hemispherical transmission and reflection measurements in the infrared. With these data, a quantitative model has been established which predicts the thermal conductivity of polyimide foams as a function of density, gas pressure and temperature. In addition the influence of low emissivity foils integrated into low density polyimide foams on the thermal conductivity has been calculated using a three-flux model of combined radiation and solid/gas conduction. Copyright © 1996 Elsevier Science Ltd.

1. INTRODUCTION

The installation of a network of measurement stations on the surface of Mars is presently investigated jointly by NASA and ESA. The Mars environment is characterized by large daily and seasonal temperature fluctuations in a low density atmosphere with carbon dioxide as its main constituent. Typical environmental conditions range between 200 and 600 Pa for the ambient pressure and between 138 and 303K for the ambient temperature [1].

The measurement stations are foreseen to be powered by solar arrays of limited size. Hence rational energy usage is a requirement; especially efficient thermal insulations are needed under these low power/low temperature conditions. In addition, accurate mathematical models are requested, in order to design the thermal insulations reliably.

Open polyimide foams have been selected from various porous candidates. The thermal conductivity in foams is determined by the gaseous conduction within the pores, the conduction via the solid structure of the foam and by radiative transfer [2]. It is well known that the total conductivity of gas-filled foams generally shows a minimum upon variation of foam density [3]. This is due to the effect that with increasing density the radiative component of the total conductivity is reduced and the solid conduction is enhanced.

The radiative extinction properties of disperse thermal insulation materials can be determined either directly by i.r. optical measurements [4–6] or indirectly, by fitting temperature-dependent measurements of the thermal conductivity to heat transfer models [7]. Once the radiative properties are known for evacuated open foam insulations the solid conductivity can be determined by subtracting the radiative contribution from the measured total conductivity.

If the thermal conductivity of a foam with given density is known as a function of gas pressure, a parameter $p_{1/2}$ can be extracted which depends predominantly on pore size and temperature [8]. $p_{1/2}$ can also be adapted to foams of other densities.

With such a model for the heat transfer in foams at hand few experimental data suffice to predict the total conductivity in a wide range of temperature, gas pressure and foam density. Even the influence of Al-foils implemented in the foam can be modeled accordingly.

2. THERMAL CONDUCTIVITY MEASUREMENTS OF POLYIMIDE FOAMS

2.1. *Sample description*

For the thermal conductivity measurements two identical polyimide foam samples with a nominal density of 50 kg m^{-3} were used. The foams have completely open cells. They have been manufactured by the company Illbruck/Switzerland by unidirectional compression of low density polyimide foams ($\rho = 8 \ldots 10$ kg m^{-3}) to the nominal density. The diameter of the samples was 200 mm and the mean mass per area m'' 1.04 kg m^{-2}. The thickness, d, was 20.2 mm at 0.1 bar external load and the corresponding density 51.3 ± 0.3 kg m^{-3}.

NOMENCLATURE

A	heater area
a	specific absorption coefficient
d	insulation thickness
D	distance between foils
E	effective extinction coefficient
e^*	effective specific extinction coefficient
$f_R(\Lambda T)$	Rosseland weight function
k_r	radiative heat transfer coefficient
l	mean free path
m''	mass per area
n	effective index of refraction of foam
p_{gas}	gas pressure
$p_{1/2}$	characteristic gas pressure
P_{el}	heater power
s^*	effective specific scattering coefficient
T	temperature
T_1, T_2	boundary temperatures
T_m	arithmetic mean temperature
T_r	radiative mean temperature.

Greek symbols

β	coefficient depending on gas properties
ΔT	temperature difference
ε	emissivity
ε^*	effective emissivity
λ_{evac}	conductivity of the evacuated specimen
λ_{gas}	gaseous conductivity
λ^0_{gas}	thermal conductivity of free gas
λ_r	radiative conductivity
λ_s	solid conductivity
λ^0_s	conductivity of nonporous material
λ_{sg}	combined solid and gaseous conductivity
Λ	wavelength
ρ	insulation density
ρ_0	density of solid material
σ	Stefan–Boltzmann constant
τ_0	optical thickness
ω_0	effective albedo
$\varnothing$	pore size.

2.2. *Test procedure*

The thermal conductivity measurements have been performed in our evacuable, externally load-controlled, guarded hot plate apparatus LOLA 3 [9], that can be operated at mean temperatures between 80 and 1100K, internal gas pressures between 10^{-3} and 10^5 Pa and external loads from 1 to 4 bar for circular shaped samples with a diameter of 200 mm and thicknesses from 1 to 28 mm. Different emissivities of the boundaries may be established.

The thermal conductivity of the polyimide samples was measured as function of internal gas pressure p_{gas} and mean temperature T in the temperature range 173–328K. Liquid nitrogen was used as cooling fluid for cold side temperature below 253K. As carbon dioxide could not be employed as a pore gas at lower temperatures due to condensation, argon was used for gas pressure dependent conductivity measurements for temperatures $T = 243$ and 173K. Surface emissivity of the adjacent plates ε has been 0.78.

The temperature difference between hot and cold plates was $\Delta T = 40$K. In order to obtain a higher accuracy and to eliminate small but unknown thermal losses between the central hot plate and the guard rings, additional measurements were performed with a temperature difference $\Delta T = 20$K. Using a simple correction procedure [9] from both ΔT measurements a more accurate thermal conductivity value can be derived. The obtained corrections are in the same range or smaller than the size of the symbols depicted in the figures. Overall uncertainties and measurement errors are 7% at most.

Temperature measurements in the apparatus are performed with Pt-100 resistors, which have been individually calibrated. Measurements of gas pressure are done with capacitance manometers (MKS Baratron Typ 220, 0–1000 Pa and 0–10^5 Pa) which are independent of the kind of gas in the apparatus. The error in gas pressure measurement in the range between 200 and 600 Pa is below 10 Pa.

The thermal conductivity is calculated from the heater power P_{el} fed into the central part with area A of the heater plate, the mean sample thickness d and the temperature difference ΔT between heater and cold plates:

$$\lambda = \frac{P_{el} \cdot d}{2 \cdot A \cdot \Delta T} \tag{1}$$

(the factor of 2 is for the symmetric arrangement of the two samples).

2.3. *Results*

2.3.1. *Thermal conductivity of the evacuated and argon filled sample as function of temperature.* In order to separate the solid and radiative conductivity of the polyimide foams, the thermal conductivity λ_{evac} of the evacuated samples was measured between mean temperatures of 150 and 300K (Fig. 1). From independently measured extinction data of the polyimide foam (see Section 3), the radiative conductivity was calculated and then subtracted from λ_{evac}. The resulting solid conductivity is also shown in Fig. 1. At room temperature the total conductivity of the evacuated sample is 3.6×10^{-3} W(mK)$^{-1}$. Here radiative transfer with about 2.6×10^{-3} W(mK)$^{-1}$ is the main heat

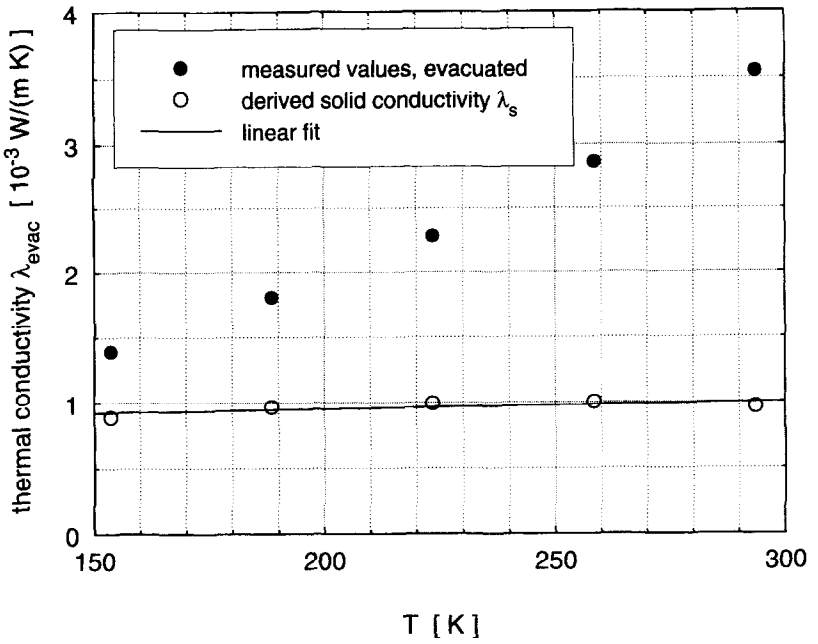

Fig. 1. Thermal conductivity λ of evacuated polyimide foam ($\rho = 50$ kg m^{-3}) as function of mean temperature T and derived solid conduction λ_s.

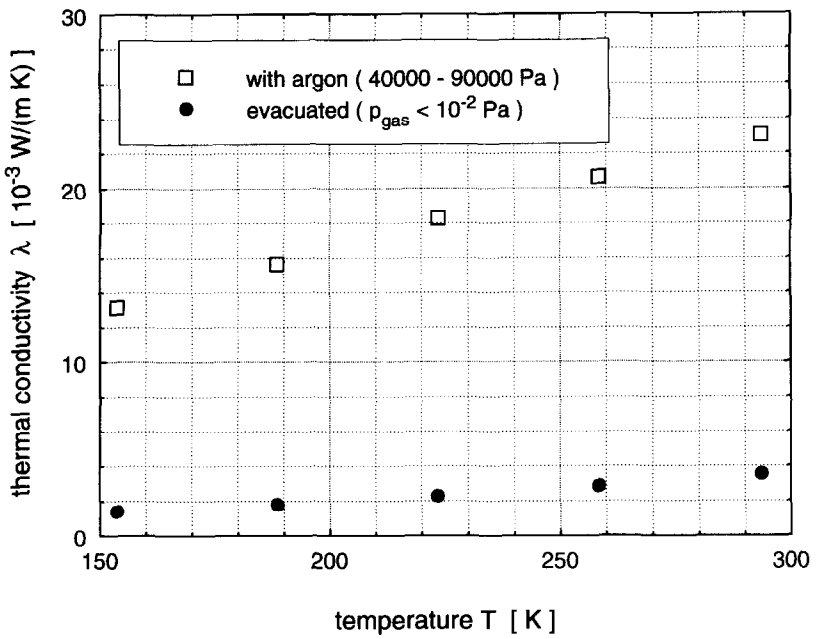

Fig. 2. Thermal conductivity λ of argon-filled polyimide foam ($\rho = 50$ kg m^{-3}) as a function of temperature T in comparison with evacuated sample.

transport mechanism, whereas solid conductivity amounts to about 1×10^{-3} W(mK)$^{-1}$. At 150K mean temperature the radiative conductivity is reduced to about 0.4×10^{-3} W(mK)$^{-1}$, while the solid conductivity is still in the order of 1×10^{-3} W(mK)$^{-1}$.

The thermal conductivity has also been measured at relatively high gas pressures of argon (above 40 000 Pa) where the gaseous conductivity is fully developed. In Fig. 2 the thermal conductivity of the argon-filled sample and the evacuated sample are compared. The fully developed gas conductivity is about a factor of five higher than the conductivity λ_{evac} of the evacuated foam.

2.3.2. *Thermal conductivity as function of gas pressure.* The foam will be exposed to a CO_2 gas pressure between 200 and 600 Pa if used as an insulation material for the Mars lander. The onset and variation of the gaseous conductivity as a function of gas pres-

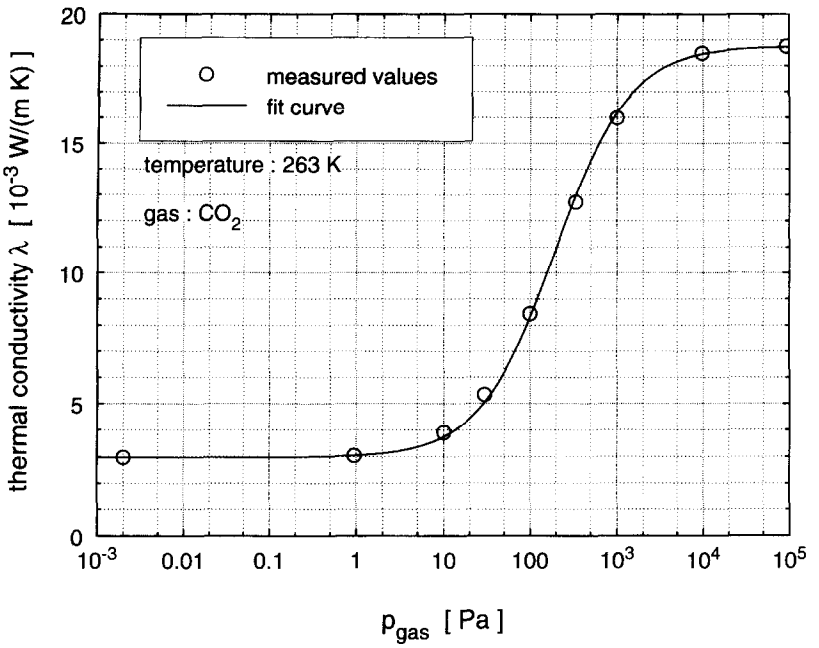

Fig. 3. Thermal conductivity λ of polyimide foam ($\rho = 50$ kg m^{-3}) as a function of CO_2 gas pressure.

sure, depends on the pore size of the foam. Figure 3 shows the measured thermal conductivity in a CO_2 atmosphere at a temperature of 263K. As can be seen, the onset of gaseous conductivity occurs at CO_2 pressures of 5 Pa. Between 50 and 1000 Pa the total conductivity varies in a wide range between 6×10^{-3} W(mK)$^{-1}$ and 16×10^{-3} W(mK)$^{-1}$. At the nominal gas pressures of 200 and 600 Pa, the gaseous conductivity has reached already more than 50% of the fully developed gas conductivity λ^0_{gas}.

At temperatures of $T = 283$ and 328K additional conductivity measurements were performed with CO_2 gas pressures of 200 Pa, 600 Pa and above 10000 Pa. The results are depicted in Fig. 4. For lower temperatures argon has to be used. As can be seen in Fig. 4 at $T = 173$K the thermal conductivity varies between 8×10^{-3} and 11×10^{-3} W(mK)$^{-1}$ in argon atmosphere with gas pressures between 200 and 600 Pa.

3. INFRARED-OPTICAL MEASUREMENTS OF SPECIFIC THERMAL RADIATION EXTINCTION

The radiative conductivity depends on the mass specific effective extinction coefficient e^*. Besides absorption the extinction coefficient e^* takes into account forward scattering by using a proper scaling procedure [4]. It can be obtained experimentally by hemispherical transmission and reflection measurements in the infrared.

3.1. *Procedure*

A gold-coated integrating sphere with 100 mm diameter was used in combination with an i.r.-Fourier-spectrometer (Bruker IFS 66v) [4]. Spectral measurements of hemispherical transmission and reflection were performed in the wavelength range 2–20 μm.

Via a three flux model for the radiative transfer in disperse media the spectral transmission and reflection data allow to determine the effective albedo ω_0, the ratio of scattering to total extinction and the effective specific extinction e^* as function of wavelength Λ [4].

For wavelengths above 20 μm usually scattering is negligible and the extinction coefficient is obtained without the integrating sphere by measuring the transmission of the direct beam. Such direct extinction measurements have been performed for wavelengths up to 200 μm. Samples of 13 mm diameter are cut from the foam with a punch. The sample thickness varies between 1 and 3 mm. Several samples of different thicknesses were measured and a mean value of extinction was derived. The accuracy of the i.r.-measurements is in the range of $\pm10\%$–$\pm20\%$ depending on the wavelength.

3.2. *Results*

Samples of density 30, 50 and 80 kg m^{-3} have been measured. In Fig. 5 the obtained effective spectral specific extinction $e^*(\Lambda)$ of the 30 and 80 kg m^{-3} samples are compared. If the microstructural properties do not vary with density (e.g. in fiber materials) it is expected that the specific extinction e^* is independent of density ρ. Especially at wavelengths below 3.5 μm, however, a significant enhancement of the spectral extinction efficiency of the 30 kg m^{-3} sample in comparison to the 80 kg m^{-3} sample can be noticed. This clearly demonstrates the differences in microstructural properties between both foam densities.

The samples of different densities are produced by

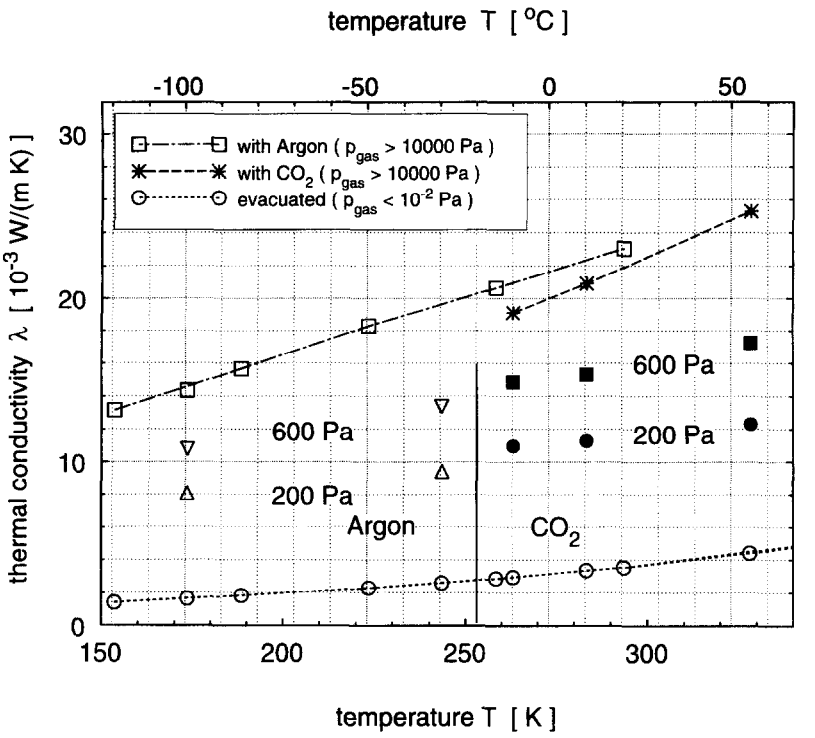

Fig. 4. Thermal conductivity λ of polyimide foam ($\rho = 50$ kg m^{-3}) in argon and CO_2 atmosphere at various gas pressures p_{gas} and temperatures T.

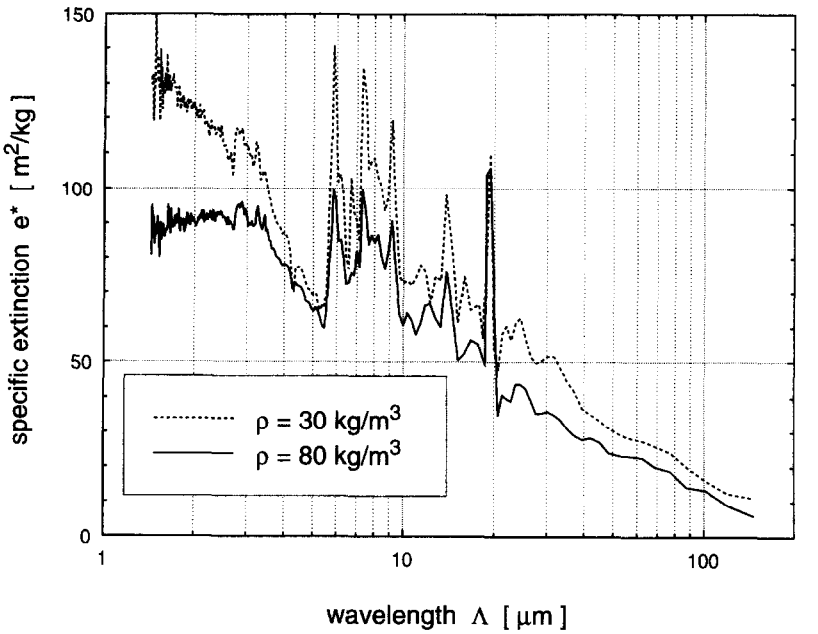

Fig. 5. Spectral specific extinction e^* for samples of density $\rho = 30$ kg m^{-3} and $\rho = 80$ kg m^{-3}.

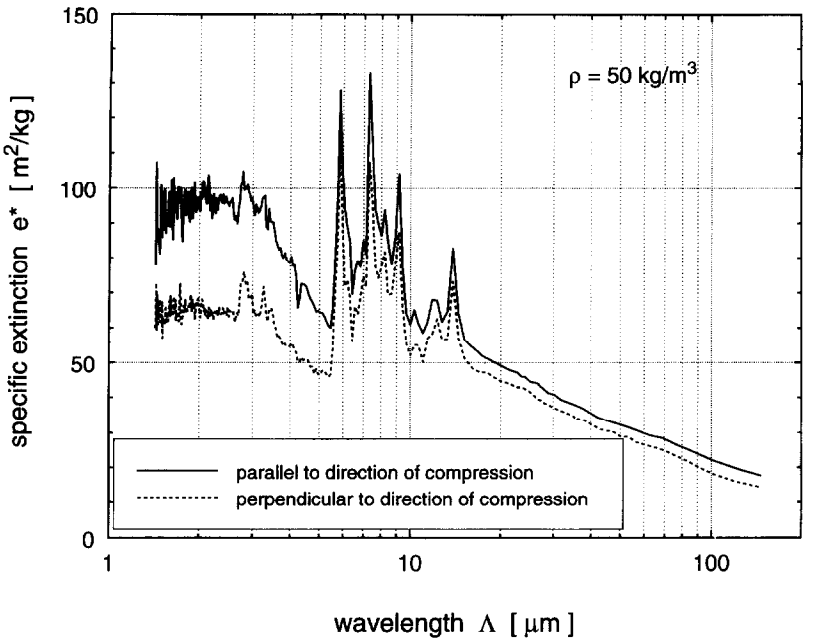

Fig. 6. Spectral specific extinction e^* of the $\rho = 50$ kg m^{-3} sample.

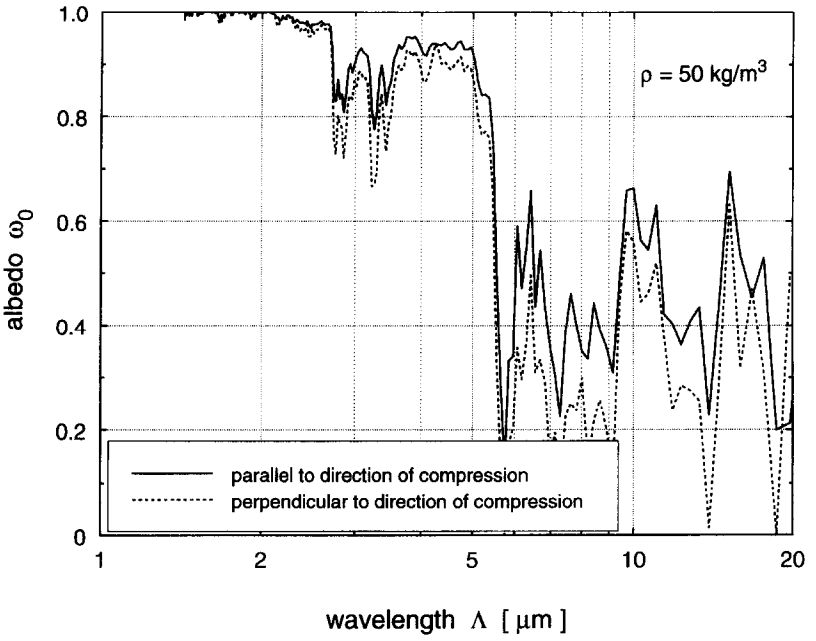

Fig. 7. Spectral albedo ω_0 of polyimide foam ($\rho = 50$ kg m^{-3}).

compressing a low density polyimide foam with an initial density of 8 kg m^{-3}. Due to the uniaxial compression the specific extinction $e^*(\Lambda)$ may also vary with the direction of measurement (parallel and perpendicular to the compression direction).

In Fig. 6 the results of spectral extinction measurements of the 50 kg m^{-2} sample in both directions are compared. A remarkable decrease of the extinction by about 30% for the perpendicular direction can be seen for wavelengths below 5 μm. From the albedo ω_0, as depicted in Fig. 7, the specific scattering coefficient $s^* = \omega_0 \cdot e^*$ (Fig. 8) and absorption coefficient $a = (1 - \omega_0) \cdot e^*$ were also obtained. As expected, the absorption (Fig. 9) does not vary with the measurement direction. From these absorption and scattering features it can be concluded that the uniaxial compression influences the scattering properties perpendicular and parallel to the compression as well as the geometry of the foam cells in a different way. The higher extinction occurs parallel to the heat flux in the conductivity measurements.

The wavelength dependent data are averaged using

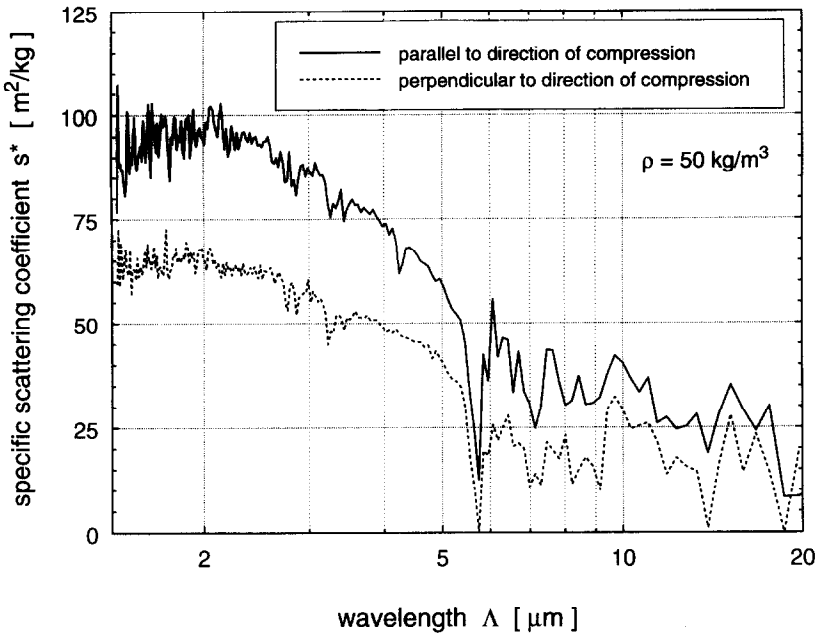

Fig. 8. Spectral specific scattering coefficient s^* of polyimide foam ($\rho = 50$ kg m^{-3}) depending on direction.

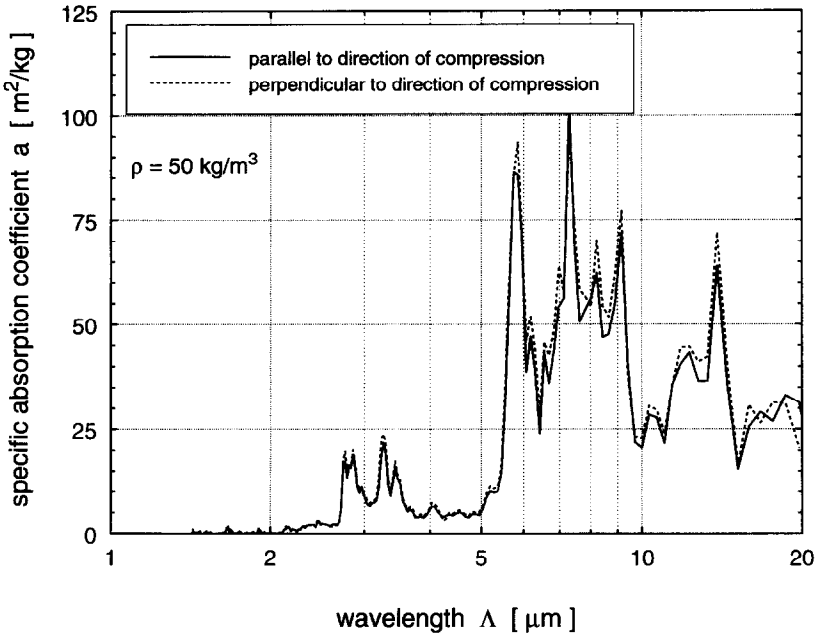

Fig. 9. Spectral specific absorption coefficient a of polyimide foam ($\rho = 50$ kg m^{-3}).

the Rosseland mean function [10] resulting in a temperature dependent extinction coefficient. The mean specific extinction e^* of the 50 kg m^{-3} sample varies between 45 and 65 m^2 kg^{-1} at temperatures between 100 and 300K (Fig. 10). The specific extinction measured perpendicular to the direction of compression is about 10% lower.

4. DATA ANALYSIS AND QUANTITATIVE DESCRIPTION OF HEAT TRANSFER IN POLYIMIDE FOAMS

Let us first consider optically thick foams where in a good approximation the three heat transfer modes—solid, gaseous and radiative conduction—add linearly to the total heat transfer.

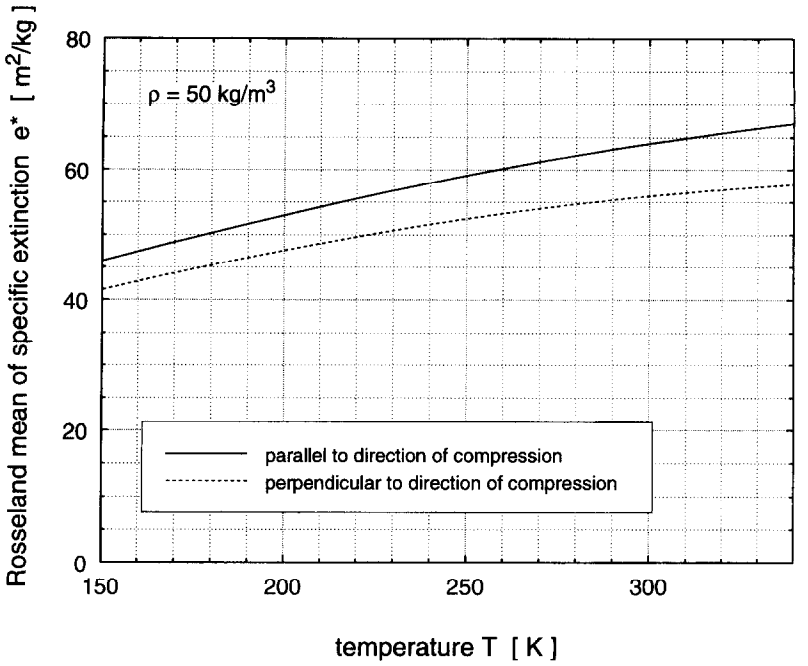

Fig. 10. Temperature dependent Rosseland mean of specific extinction $e^*(T)$ of polyimide foam ($\rho = 50$ kg m^{-3}).

4.1. *Gaseous thermal conductivity of the gas in the pores*

In general the ratio of the mean free path of the gas molecules l and the pore size Φ determines the gaseous conductivity λ_{gas} according to:

$$\lambda_{gas} = \frac{\lambda^0_{gas}}{1 + 2\beta \dfrac{l(T, p_{gas})}{\varnothing(\rho)}} \tag{2}$$

with λ^0_{gas}: conductivity of free gas; β: coefficient depending on gas properties and gas/wall interaction; $\varnothing(\rho)$: pore diameter (function of foam density).

Literature data of free gaseous conductivity λ^0_{gas} of argon and CO_2 were taken from Touloukian [11]. For temperatures between 170 and 350K the gaseous conductivity was approximated by the following linear fits:

$$\lambda^0_{CO_2}(T)/(\mathrm{W(mK)^{-1}}) = -0.0044 + 69.4 \times 10^{-6} \cdot T/(\mathrm{K}),$$

$$\lambda^0_{Ar}(T)/(\mathrm{W(mK)^{-1}}) = 0.0017 + 53.7 \times 10^{-6} \cdot T/(\mathrm{K}). \tag{3}$$

The mean free path l of a free gas is inversely proportional to the gas pressure p_{gas}. For a fixed temperature T thus the gaseous conductivity as a function of gas pressure can be described by:

$$\lambda_{gas}(p_{gas}, T) = \lambda^0_{gas}(T) \cdot \left(1 + \frac{p_{1/2}(T)}{p_{gas}}\right)^{-1}. \tag{4}$$

For $p_{gas} = p_{1/2}$ half of the gaseous conductivity of the free gas has developed. The constant $p_{1/2}$ is fitted to the experimental data. According to Fig. 3 $p_{1/2} \approx 200$ Pa is obtained for CO_2 as filling gas and a temperature of 263K.

The characteristic pressures $p_{1/2}$ of CO_2 and argon have been derived from the experimental data as a function of temperature T (see Fig. 11). The temperature dependent characteristic pressure is compared to data for the mean free path l of CO_2 ($l \propto \eta/\rho \cdot T^{-0.5}$), which have been calculated using literature data of the viscosity η [12].

Assuming that $p_{1/2}$ is proportional to the mean free path l as depicted, one obtains the following functional dependences of $p_{1/2}$ as a function of temperature T:

$$p_{1/2}(CO_2)/\mathrm{Pa} = 1.48 \cdot (T/(\mathrm{K}) - 94.6) \quad \text{for } CO_2,$$

$$p_{1/2}(\mathrm{Ar})/\mathrm{Pa} = 1.54 \cdot (T(\mathrm{K}) - 33) \quad \text{for argon.} \tag{5}$$

In the case of CO_2 for temperatures below 250K no experimental data exist; thus there may be a considerable deviation from this relation below 250K.

4.2. *Radiative conductivity*

The radiative conductivity λ_r in optically thick media (optical thickness $\tau_0 \gg 1$) according to diffusion theory [10] is:

$$\lambda_r = \frac{16}{3}\sigma n^2 \frac{T^3}{E^*(T)} = \frac{16}{3}\sigma n^2 \frac{T^3}{e^*(T) \cdot \rho} \tag{6}$$

with $E^*(T)$: effective extinction coefficient $= e^* \cdot \rho$; n: effective index of refraction of the foam ($n^2 \approx 1.05$); σ: Stefan–Boltzmann constant.

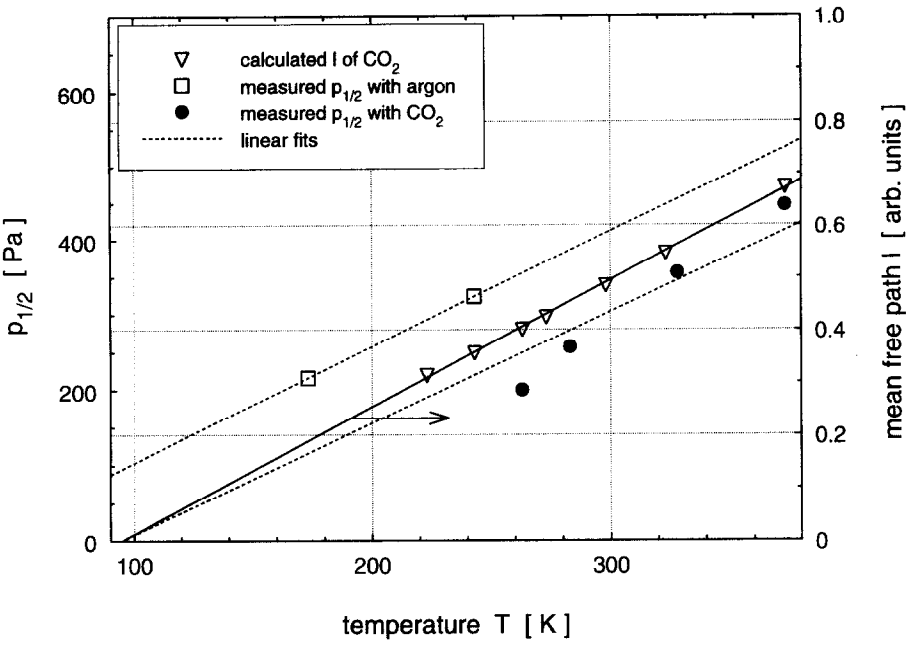

Fig. 11. Measured characteristic gas pressure $p_{1/2}$ of Ar and CO_2 in polyimide foam as a function of temperature T and calculated temperature dependent mean free path l for CO_2.

In non-gray media the mass specific extinction coefficient $e^*(T)$ is obtained by integrating the spectral extinction with the Rosseland weight function $f_R(\Lambda T)$:

$$\frac{1}{e^*(T)} = \int \frac{f_R(\Lambda T)}{e^*_\Lambda} \mathrm{d}\Lambda. \tag{7}$$

For the calculation of the radiative conductivity of the 50 kg m^{-3} sample according to Fig. 10 the following temperature dependence is used:

$$e^*(T)/(\mathrm{m^2 kg^{-1}}) = 17.4 + 0.229 \cdot T(\mathrm{K}) - 2.27 \times 10^{-4} \cdot T^2(\mathrm{K^2}). \tag{8}$$

In the case of highly emitting boundaries ($\varepsilon > 0.5$) and optically thin foams the following equation may also be used as a good approximation:

$$\lambda_r = \frac{16}{3} \sigma n^2 \frac{T^3}{\frac{4}{3D} + E^*} (\varepsilon > 0.5), \tag{9}$$

with D: distance between boundaries (foils). The optical thickness $\tau_0 = E^* \times D$ here may vary between 0 and infinity.

4.3. *Solid conductivity of foam*

In a simple model the foam solid conductivity λ_s may be derived by:

$$\lambda_s = \frac{1}{3} \lambda_s^0 \frac{\rho}{\rho_0}, \tag{10}$$

where λ_s^0 is the thermal conductivity of the nonporous polyimide material, ρ_0 its density and ρ the density of the foam (with $\rho \ll \rho_0$). If we subtract the radiative conductivity λ_r according to equation (6) from the measured conductivity λ_{evac} of the evacuated 50 kg m^{-3} foam, we obtain the solid conductivity with about 0.001 W(mK)$^{-1}$ as shown in Fig. 1.

4.4. *Total conductivity of polyimide foam*

The total conductivity of the polyimide foam now can be calculated as the sum of λ_s, λ_{gas} and λ_r:

$$\lambda(\rho, T, p_{gas})/(\mathrm{W(mK)^{-1}}) = 0.001 \frac{\rho/(\mathrm{kg\,m^{-3}})}{50} + 1.15 \frac{\lambda^0_{gas}(T)/(\mathrm{W(mK)^{-1}})}{1 + \frac{p_{1/2}}{p_{gas}(T)}} + \frac{16}{3} \frac{\sigma T^3/\mathrm{K^3}}{e^*(T)/(\mathrm{m^2\,kg^{-1}}) \cdot \rho/(\mathrm{kg\,m^{-3}})}, \tag{11}$$

with $e^*(T)$ according to equation (7), $\lambda^0_{gas}(T)$ and $p_{1/2}(T)$ according to equations (2) and (4).

Due to nonlinear interactions between solid and gaseous conduction the second term has been corrected by the factor 1.15 extracted from the experimental data. This interaction generally is far stronger especially in powder insulations, where, for gas pressures beyond 1000 Pa a linear superposition of the three heat transfer modes is not valid any longer [13].

The relative contributions of solid, gaseous and radiative conductivities to the total conductivity of the polyimide foam with density $\rho = 50$ kg m^{-3} are

Table 1. Thermal conductivity λ [10^{-3} W(mK)$^{-1}$] of a 8 kg m^{-3} polyimide foam with Al-foils ($\varepsilon = 0.1$) separated by a distance of 5 mm in a CO_2 atmosphere; effective emissivity $\varepsilon^* \approx 0.5 \ldots 0.6$

p_{gas} [Pa]	T [K] 173	243	283	328
0	1.1	2.2	3.1	4.3
200	13.1	17.9	21.2	25.7
600	13.8	19.3	22.9	27.6

depicted in Table 2 for temperatures $T = 173$ and 283 K and pressures $p_{gas} = 200$ and 600 Pa, for a CO_2 atmosphere. In all cases the gaseous conductivity within the foam dominates the total conductivity with percentages ranging from 70 to 82%.

4.5. *Influence of low emissivity separation foils within polyimide foam*

Low emittance aluminized plastic foils are used as radiation barriers in highly efficient vacuum insulations. In low density polyimide foams ($\rho = 8$ kg m^{-3}) radiation may constitute a major part of the heat transfer. In the following we thus examine the heat transfer for a combination of foils and low density foam.

The radiative heat transfer coefficient k_r between two surfaces with the emissivity ε is:

$$k_r = \frac{4\sigma T^3}{\frac{2}{\varepsilon} - 1}. \tag{12}$$

If a nonabsorbing material of optical thickness τ_0 is introduced between the foils, the different heat transfer modes (gaseous and solid conduction and radiation) add up linearly to the total heat transfer coefficient k. For a stack of foils with separation distance D one gets:

$$k = \frac{\lambda_{sg}}{D} + \frac{16}{3}\frac{\sigma T^3}{\frac{4}{3}\left(\frac{2}{\varepsilon} - 1\right) + \tau_0}, \quad (\omega_0 = 1) \tag{13}$$

with λ_{sg}: combined solid and gaseous conduction. This equation, however, is only valid for a nonabsorbing, scattering medium between the foils!

If an absorbing material (albedo $\omega_0 < 1$) separates the foils, the total heat transfer increases. This is attributed to enhanced conduction close to the boundaries due to a large temperature gradient and successive emission and reabsorption of radiative flux by the medium.

It has been shown that a three flux solution of the equation of transfer can describe the total heat transfer for arbitrary values of albedo ω_0 and optical thickness τ_0 with high accuracy [7]:

$$k = \frac{(\lambda_{sg} + \lambda_r)}{D} \cdot \left[1 + \frac{1}{\frac{\lambda_{sg}}{\lambda_r}\frac{p\tau_0}{2}\coth\left(\frac{p\tau_0}{2}\right) + \frac{\frac{3}{4}\tau_0\left(1 + \frac{\lambda_{sg}}{\lambda_r}\right)}{\frac{2}{\varepsilon} - 1}} \right]^{-1}, \quad (\omega_0 \leqslant 1) \tag{14}$$

with:

$$p = \frac{3}{2}\sqrt{\frac{1 - \omega_0}{1 - \omega_0/4}\left(1 + \frac{\lambda_r}{\lambda_{sg}}\right)}$$

and

$$\lambda_r = \frac{16}{3} n^2 \sigma \frac{T^3 D}{\tau_0}.$$

An 'effective emissivity' ε^* can be defined, if it is chosen in such a way that $\lambda_{add}(\varepsilon^*) = \lambda_{exact}(\varepsilon)$, with $\lambda_{add} = k \cdot D$ according to equation (13) and λ_{exact} according to equation (14). The effective emissivity ε^* is larger than ε for absorbing media and only in the case $\omega_0 = 1$ one gets $\varepsilon^* = \varepsilon$. In non-gray media τ_0 and ω_0 are dependent on wavelength Λ. Equation (14) then has to be integrated with the Rosseland function $f_R(\Lambda T)$ as weight:

$$k = \int f_R(\Lambda T) \cdot k(\tau_{0,\Lambda}, \omega_{0,\Lambda})\, d\Lambda. \tag{15}$$

The above equations now can be used to determine the total heat transfer in a system made up of foils of emissivity ε and polyimide foam layers. As input for the combined solid and gaseous conductivity λ_{sg} we used the first and second expressions of equation (11). For the optical thickness $\tau_0 = e^*(\Lambda) \cdot \rho \cdot D$ and albedo $\omega_0(\Lambda)$ we used the values of the i.r.-optical measure-

Table 2. Contribution of different heat transfer modes to total conductivity of polyimide foam ($\rho = 50$ kg m^{-3}) for $T = 173$, 283K and CO_2 gas pressure $p_{gas} = 200$, 600 Pa

	Relative contributions Solid conductivity	Gas conductivity	Radiation	Total conductivity [10^{-3} W(mK)$^{-1}$]
$T = 173$K, $p = 200$ Pa	13.9%	77.3%	8.8%	7.2
$T = 173$K, $p = 600$ Pa	11.1%	81.8%	7.0%	9.0
$T = 283$K, $p = 200$ Pa	9.6%	69.9%	20.5%	10.5
$T = 283$K, $p = 600$ Pa	6.6%	79.2%	14.2%	15.1

Table 3. Contribution of different heat transfer modes to total conductivity of polyimide foam ($\rho = 8$ kg m^{-3}) with aluminized foils ($D = 5$ mm, $\varepsilon = 0.1$); gas: CO_2

	Relative contributions			Total conductivity
	Solid conductivity	Gas conductivity	Radiation	[10^{-3} W(mK)$^{-1}$]
$T = 173$K, $p = 200$ Pa	1.7%	83.5%	14.8%	9.6
$T = 173$K, $p = 600$ Pa	1.6%	84.3%	14.1%	10.1
$T = 283$K, $p = 200$ Pa	0.8%	72.0%	27.2%	19.9
$T = 283$K, $p = 600$ Pa	0.7%	74.4%	24.9%	22.0

Table 4. Contribution of different heat transfer modes to total conductivity of polyimide foam ($\rho = 8$ kg m^{-3}) without foils; gas: CO_2

	Relative contributions			Total conductivity
	Solid conductivity	Gas conductivity	Radiation	[10^{-3} W(mK)$^{-1}$]
$T = 173$K, $p = 200$ Pa	1.3%	66.5%	32.2%	12.1
$T = 173$K, $p = 600$ Pa	1.3%	67.8%	30.9%	12.5
$T = 283$K, $p = 200$ Pa	0.6%	51.8%	47.6%	27.8
$T = 283$K, $p = 600$ Pa	0.5%	54.9%	44.6%	29.8

ments as depicted in Figs. 6 and 7, correlated to 'parallel to direction of compression'.

Calculations with the wavelength dependent values $e^*(\Lambda)$ and $\omega_0(\Lambda)$ have been performed with foam density 8 kg m^{-3} and foils of emissivity $\varepsilon = 0.1$. Table 1 shows the results for a foil distance of 5 mm and temperatures between 173 and 328K.

The relative contributions of solid, gaseous and enhanced radiative modes to the total heat transfer for the low density foam with ($D = 5$ mm) and 'without foils' ($D = 100$ mm) are depicted in Tables 3 and 4 for temperatures $T = 173$ and 283K and CO_2 gas pressures $p_{gas} = 200$ and 600 Pa. The pressure dependence in CO_2 atmosphere is shown in more detail in Fig. 12 ($T = 283$K) and Fig. 13 ($T = 173$K). In the case of a low density pure polyimide foam one notes, according to Fig. 12 for $T = 283$K and $p_{gas} \geqslant 200$ Pa, that the radiative heat transfer is about one half of the total. After introduction of aluminized foils ($D = 5$ mm, $\varepsilon = 0.1$) this radiative flux is reduced only by a factor of two. The overall reduction of the thermal transport however, is even less, i.e. about 25%.

For low temperatures $T = 173$K and $p_{gas} \geqslant 200$ Pa the aluminized foils reduce the thermal transport by

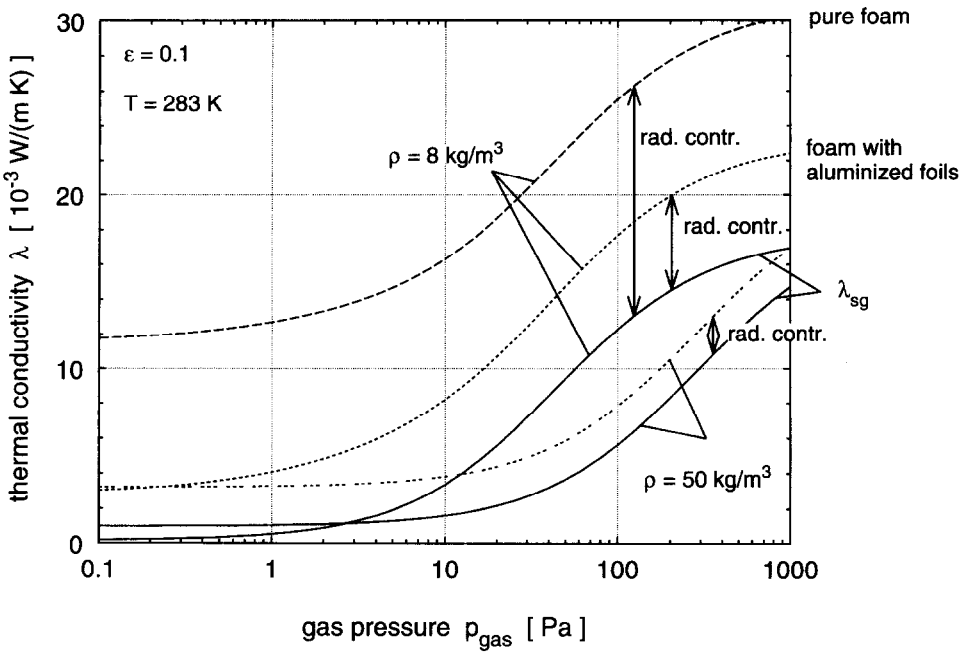

Fig. 12. Calculated gas pressure dependent thermal conductivity for $\rho = 8$ kg m^{-3} polyimide foam at $T = 283$K without and with integrated aluminized foils ($\varepsilon = 0.1$) and of $\rho = 50$ kg m^{-3} foam for comparison.

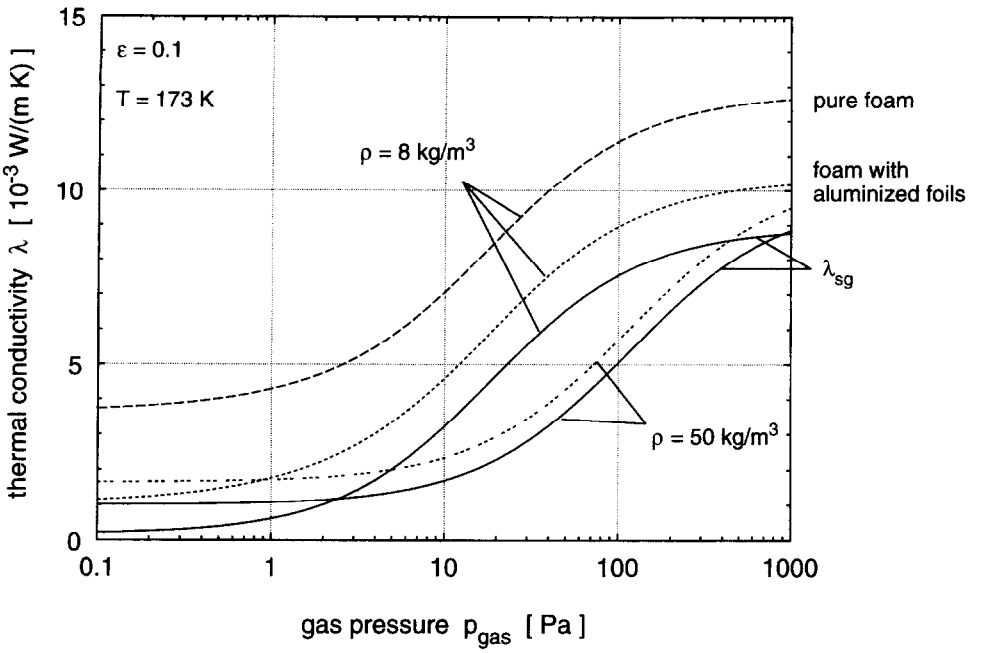

Fig. 13. Calculated gas pressure dependent thermal conductivity for $\rho = 8$ kg m^{-3} polyimide foam at $T = 173$K without and with integrated aluminized foils ($\varepsilon = 0.1$) and of $\rho = 50$ kg m^{-3} foam for comparison.

some 15% compared to the pure foam (see Fig. 13). In this case foils become even less effective.

In the case of the high density foam ($\rho = 50$ kg m^{-3}) the influence of gas pressure on thermal conductivity in the range between 200 and 600 Pa is dominant while the radiative conductivity gives a relatively small contribution as also depicted above in Table 2.

5. CONCLUSIONS

The parameters describing the heat transfer of polyimide foam samples have been determined experimentally. With these data and an appropriate heat transfer model, the thermal transport can be calculated for arbitrary temperatures, gas pressures and foam density. It is even possible to model the influence of low emissivity foils on the heat transfer. Thus the thermal performance of different designs (variations of density, integration of foils) can be evaluated even without performing additional time consuming experiments.

REFERENCES

1. W. P. P. Fischer, W. D. Ebeling, B. Haase and K. Keller, Porous insulation performance under martian environment, ICES-932116. In: *23rd Int. Conf. on Environmental Systems*, Colorado Springs, Colorado, 12–15 July (1993).
2. J. Kuhn, H. P. Ebert, M. C. Arduini-Schuster, D. Büttner and J. Fricke, Thermal transport in polystyrene and polyurethane foam insulations, *Int. J. Heat Mass Transfer* **35**, 1795–1801 (1992).
3. L. Glicksman, M. Schütz and M. Sinofsky, Radiation heat transfer in foam insulations, *Int. J. Heat Mass Transfer* **30**, 187–197 (1987).
4. J. Kuhn, S. Korder, M. C. Arduini-Schuster, R. Caps and J. Fricke, Infrared optical transmission and reflection measurements on loose powders, *Rev. Sci. Instrum.* **64**, 2523–2530 (1993).
5. J. Kuhn, G. Göbel, S. Korder, M. C. Arduini-Schuster and J. Fricke, Infrared-optical properties of insulating powders, *High Temp. High Press.* **25**, 343–351 (1993).
6. R. Caps, M. C. Arduini-Schuster, H. P. Ebert and J. Fricke, Improved thermal radiation extinction in metal coated polypropylene microfibers, *Int. J. Heat Mass Transfer* **36**, 2789–2794 (1993).
7. J. Fricke and R. Caps, Heat transfer in thermal insulations—recent progress in analysis, *Int. J. Thermophys.* **9**, 885–895 (1988).
8. M. G. Kaganer, *Thermal Insulation in Cryogenic Engineering*. Israel Program for Scientific Translation, Jerusalem (1969).
9. U. Heinemann, J. Hetfleisch, R. Caps, J. Kuhn and J. Fricke, Evacuable guarded hot plate for thermal conductivity measurements between −200°C and 800°C, *Eurotherm seminar No.* 44, Lisbon (1995).
10. H. C. Hottel and A. F. Sarafim, *Radiative Transfer*. McGraw-Hill, New York (1967).
11. Y. S. Touloukian, P. E. Liley and S. C. Saxena, *Thermal Conductivity—Nonmetallic Liquids and Gases*, 1st Edn, Vol. 3 of *Thermophysical Properties of Matter Data Series*, p. 4 and p. 147. Plenum Press, New York (1970).
12. R. C. Weast, M. J. Astle and W. H. Beyer, *Handbook of Chemistry and Physics*, 65th Edn, p. F42. CRC Press, Boca Raton, FL (1984).
13. C. Stark and J. Fricke, Improved heat-transfer models for fibrous insulations, *Int. J. Heat Mass Transfer* **36**, 617–625 (1993).